8-7-2024

Hydrologic Disturbances and Land Cover: A Study on Stream Metabolism Dynamics

Deandre Presswood

Hydrologic Disturbances and Land Cover: A Study on Stream Metabolism Dynamics

by

Deandre Presswood

Under the Direction of Sarah H Ledford, PhD

A Thesis submitted in Partial Fulfillment of the Requirements for the Degree of

Master of Science

in the College of Arts and Sciences

Georgia State University

2024

ABSTRACT

This study examines the effects of hydrologic disturbances and land cover on stream metabolism within various watersheds in the Piedmont region. I utilized continuous dissolved oxygen measurements and stream metabolism data from 14 sites, collected over a period of up to 11 years. This research builds on existing datasets to assess changes in flow and land cover impacts on gross primary productivity (GPP) and ecosystem respiration (ER). Results indicate that GPP resistance significantly decreases with flow event size, while ER resistance remains stable. GPP recovery times were longer for larger storms, showing significant differences between the highest and lower flow quartiles. Even-mixed land-cover watersheds exhibited lower GPP resistance and longer recovery times than urban and vegetated watersheds, while ER resistance and recovery did not significantly differ across land cover types. These findings underscore the importance of considering hydrologic regimes and land cover in watershed management to enhance stream resilience.

INDEX WORDS: Stream metabolism, Gross primary production, Ecosystem respiration, Resistance, Recovery, Land cover

Hydrologic Disturbances and Land Cover: A Study on Stream Metabolism Dynamics

by

Deandre Presswood

Committee Chair: Sarah H Ledford

Committee: Rachel Scarlett

Marie Kurz

Luke Pangle

Electronic Version Approved:

Office of Graduate Services

College of Arts and Sciences

Georgia State University

August 2024

ACKNOWLEDGEMENTS

TABLE OF CONTENTS

LIST OF TABLES

LIST OF FIGURES

1   INTRODUCTION

Whole-stream metabolism, the summation of all biological processes within a stream ecosystem, has become a key indicator for evaluating aquatic biological productivity and ecosystem functionality. Stream metabolism is highly responsive to environmental shifts and provides insights into the health and operational dynamics of aquatic ecosystems (Odum 1956, Trentman et al., 2022, Young et al., 2008). Historically, the analysis of diel changes in dissolved oxygen (DO) levels has been integral to assessing whole-stream metabolism and biological processes. The importance in utilizing DO data has become more pronounced in the wake of the Clean Water Act (33 U.S.C. §1251 et seq., 1972), which placed a spotlight on the management of aquatic environments. While stream metabolism data does not necessarily provide a simpler alternative to raw DO data, it enriches our understanding by offering detailed insights into the dynamics of DO production and consumption through the lenses of gross primary productivity (GPP) and ecosystem respiration (ER). This approach allows for a more granular examination of ecological processes in streams, highlighting the intricate balance between autotrophic and heterotrophic activities. Stream metabolism has been found to be controlled by light (Bernhardt et al., 2018), flow (Roley et al., 2014), nutrient availability (Hoellein et al., 2013), and human impacts (Blaszczak et al., 2019).

One of the central concepts of stream metabolism is the dynamic between light exposure and the generation of oxygen by primary producers through photosynthesis. The availability of light is influenced by various stream and watershed characteristics, notably the presence of riparian vegetation, which plays a pivotal role in attenuating sunlight, consequently, decreasing the photosynthetic potential of aquatic organisms (Bernhardt et al., 2022, Fellows et al., 2006, Hill et al., 2001). Beyond vegetation, a stream's geomorphology and geological attributes can

affect its clarity and light penetration by influencing sediment suspension and the nature of the streambed (Andreadis et al., 2020, Bott 1983). Previous studies have attempted to account for stream bed mobilization by quantifying the flow volume or stream power required to displace a streams benthic surface (Atkinson et al., 2008, Uehlinger 2006)

Land use practices adjacent to and within watersheds further drive variability in stream metabolism. Land use can impact stream metabolism by changing many of the controlling factors, including light, flow, and nutrients. Land use can disproportionality effect GPP or ER. Studies have found that photosynthetically active radiation can explain up to 90% of daily variation in GPP while changes in nutrient concentrations can largely explain daily variation in ER (Mulholland et al., 2001). Changes in the landscape, particularly through urban development, significantly alter flow regimes, leading to enhanced variability in nutrients entering streams and sediment movement—factors that directly impact metabolic rates and the communities of primary producers (Blaszczak et al., 2019, O'Driscoll et al., 2010, Walsh et al., 2005). These hydrologic changes can largely be attributed to the spread of impermeable surfaces, as extensively documented in literature (Bhaskar et al., 2016, Walsh et al., 2005). Urbanization, in particular, leads to increased stream "flashiness," a phenomenon that can displace primary producers and cause rapid sediment movement, thus influencing stream metabolism (Blaszczak et al., 2019, O'Driscoll et al., 2010, Walsh et al., 2005). Agricultural land use can have similar effects as urbanization but can often have elevated nutrients concentrations in comparison to streams in urban or highly vegetated watersheds (Bernot et al., 2010, Griffiths et al., 2013).

Hydrologic disturbances, characterized by significant changes in water discharge, are critical factors influencing the metabolic dynamics of stream ecosystems. Early research by

Young & Huryn (1996) highlighted the potential negative impacts of discharge variability on stream metabolism, setting the stage for more detailed investigations. Uehlinger (2000) furthered this work by providing a structured framework for identifying hydrologic disturbances and examining their effects on stream metabolism, emphasizing the importance of considering the unique hydrologic attributes of different regions. Bernhardt et al. (2018) discusses the multitude of possible outcomes of flow events depending on water velocity, turbidity, and antecedent conditions. Bernhardt et al. (2018) notes floods can regulate spatial and temporal patterns of many ecological processes by inputting or removing organic matter. Roley et al. (2014) showed that by restoring an agricultural floodplain, thus decreasing average flow velocity streams can become more resistant to flow events.

Recent studies have begun to emphasize the importance of resistance and recovery as key metrics to evaluate how stream metabolism responds to and recovers from disturbances. Resistance reflects the degree to which an ecosystem's metabolic rates remain stable in the face of disturbances, indicating its robustness. Conversely, recovery indicates the ecosystem's ability to return to its original metabolic state post-disturbance, capturing the speed and efficiency of its recovery. These concepts are pivotal in understanding the adaptability of stream ecosystems to environmental changes, yet their application in the context of varying land uses and hydrologic disturbances remains underexplored. Studies focusing on metabolic responses to storm events have published a varying range of results. Reisinger et al. (2017) showed metabolic responses to large storms hardly differ in urban catchments, Qasem et al. (2022) discussed how wastewater treatment plants can cause GPP and ER to increase during flood events, and O'Donnell & Hotchkiss (2022) displayed a relationship between the magnitude of isolated flow events and GPP resistance.

Work to bridge these competing metabolic drivers is still needed, particularly when considering the complex interconnections between land use and stream metabolism, an area less developed within aquatic ecology (Alberts et al., 2017, Fuß et al., 2017, Young & Huryn 1999). The nuanced impacts of hydrologic disturbances, coupled with diverse land uses on stream metabolism, are often confined to localized studies and lack a broader synthesis (Griffiths et al., 2013, Trentman et al., 2022). This oversight raises a critical question: how do stream metabolic responses to hydrologic disturbances vary across different land use scenarios? To address this, my study aims to quantify these effects by comparing stream metabolism across various degrees of watershed urbanization and assessing the role of riparian vegetation. I propose two hypotheses: (H1) Stream metabolism's resistance to disturbances decreases with increased anthropogenic land use and larger hydrologic disturbances; and (H2) Higher recovery will be related to lower anthropogenic influences during small flow events but will quickly decline as flow events increase (Fig. 1).
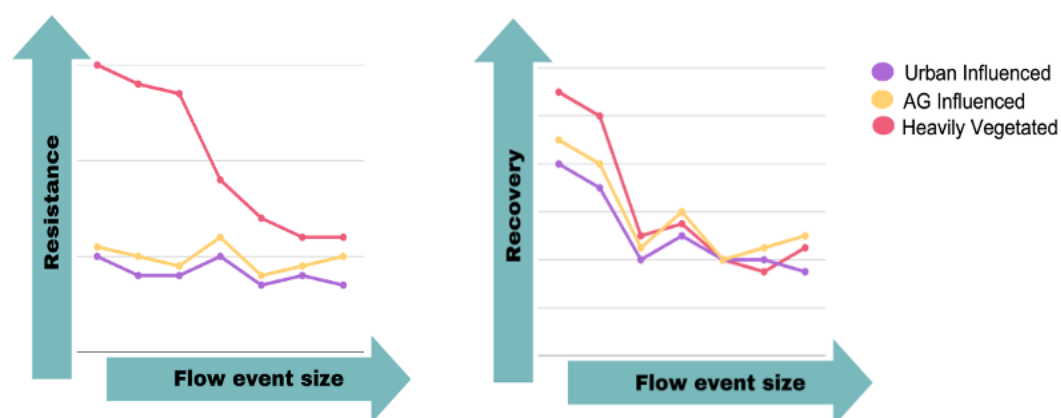
Figure 1:Visual Representation of Hypotheses

The graph displays the hypothesized trends in resistance and recovery of stream metabolism across varying flow event sizes and land cover—urban influenced, agriculturally influenced, and heavily vegetated. It supports hypothesis 1, suggesting a negative correlation between resistance and anthropogenic land cover, and hypothesis 2, where higher recovery associated with low anthropogenic impact decreases as flow events intensify. Both figures assume GPP and ER will respond similarly.

2   METHODS

2.1   Study Sites

All sites (Fig. 2) were initially modeled for stream metabolism by Appling et al. (2018b), with the earliest data spanning from 2008 to 2016. Of these, nine sites continued to be modeled by Marzolf et al. (2023), extending the data range from 2016 to 2021. Additionally, I selected two sites previously modeled by Appling that were not included in Marzolf's selection (Cornish Creek and Nancy Creek at Johnson Ferry), continuing their analysis for the period of 2016 to 2021. Sites range in watershed size from 10.9 to 491.8 km2 (Table 1).
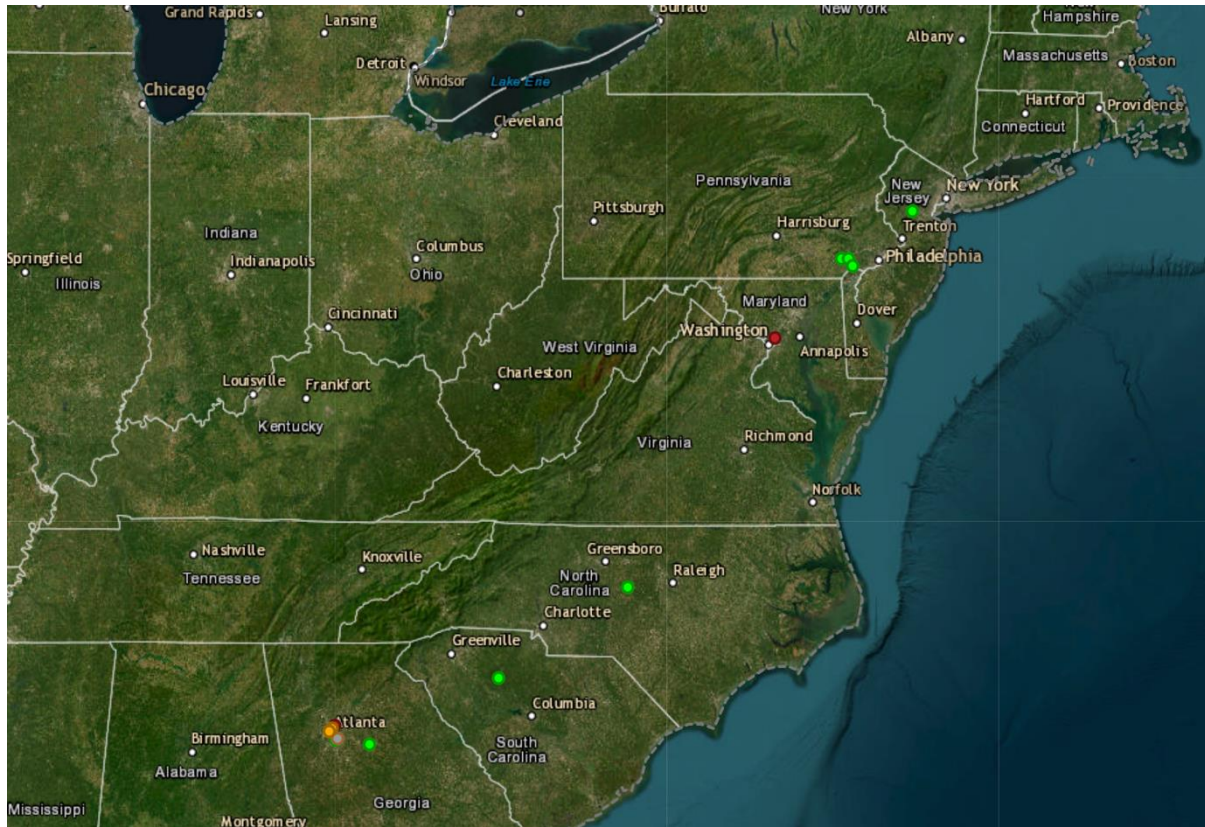
Figure 2:Site Locations In the Piedmont Physiographic Region
Pictured are all sites. Colors represent flow conditions on 02/16/2024. Green signifies high flow, orange low flow conditions, and red extreme low flow conditions.

Table 1:Number of Flow Events Captured Across Multiple Study Sites Ordered by Watershed Size (2008-2021).

This table is ordered by watershed size and contains the number of flow events captured across multiple study sites in Georgia (GA), Pennsylvania (PA), North Carolina (NC), Maryland (MD), South Carolina (SC), and New Jersey (NJ) over the years 2008-2021. It includes details on the state and USGS gage number and watershed area (in square miles) for each site.

Site	USGS Gage Number	Watershed area mi^2	Years Modeled	Events captured	Land Cover
Intrenchment Creek, GA	02203700	10.9	2008-2020	20	Urban
Proctor Creek, GA	02336526	15.7	2007-2021	69	Urban
Nancy Creek, GA	02336410	23.2	2013-2021	43	Urban
South River,GA	02203655	23.2	2009-2021	9	Urban
Cornish Creek, GA	02208493	27.6	2015-2021	50	Vegetated
Nancy Creek RB, GA	02336360	28.1	2008-2021	51	Urban
Nancy Creek WW, GA	02336410	37.5	2008-2021	44	Urban
West Branch, PA	01480617	55	2008-2021	75	Even Mixed
Rocky R, NC	02101726	69.5	2009-2021	34	Vegetated
NE Anacostia River, MD	01649500	75.0	2008-2020	66	Urban
East Branch, PA	01480870	89.7	2008-2021	99	Even Mixed
Brandywine, PA	01481000	288.1	2008-2021	71	Even Mixed
Enoree River, SC	02160700	445.1	2008-2021	13	Vegetated
Raritan River, NJ	01400500	491.8	2008-2021	54	Even Mixed

2.2   Estimating Metabolism

While numerous models exist to estimate and describe stream metabolism, many utilize measurements of DO to distinguish between the processes that produce and consume oxygen in a stream. The model I have chosen, the one-station method developed by Odum (1956), specifically correlates GPP with factors like stream depth and the availability of sunlight, which are crucial for photosynthesis. Similarly, ER is associated with stream depth, which affects oxygen availability and consumption by aquatic organisms. Additionally, the model links the reaeration constant—a measure of how oxygen moves between water and air—with water temperature and oxygen saturation levels.

Equation 1: Appling et al. (2018a)

$$\frac{dO_{i,d}}{dt} = \left(\frac{GPP_d}{\bar{Z}_{i,d}} \; X \; \frac{PPFD_{i,d}}{PPFD_d}\right) + \left(\frac{ER_d}{\bar{Z}_{i,d}}\right) + f_{i,d}(K600_d)(Osat_{i,d} - O_{i,d})$$

- $dO_{i,d}/dt$: This is the rate of change of dissolved oxygen concentration at a specific time index (i) on a particular day (d).

- GPP_d: Stands for Gross Primary Productivity on day d, which is the amount of oxygen produced by photosynthesis per square meter per day.

- $PPFD_{i,d}/PPFD_d$: This ratio compares the Photosynthetic Photon Flux Density at a specific time (i) on day (d) ($PPFD_{i,d}$) to the daily average PPFD ($PPFD_d$). It reflects how light availability at a specific time relates to the average over the day.

- ER_d: Represents the Ecosystem Respiration on day d, the rate at which oxygen is consumed by respiration across the ecosystem per square meter per day.

- $1/z_{i,d}$: The inverse of the stream depth at time i on day d, indicating that GPP and ER are influenced by the depth of the water.

- $f_{i,d}(K600_d)$: A function that modifies the daily average gas exchange rate coefficient ($K600_d$) to an O_2-specific, temperature-specific gas exchange coefficient ($KO2_{i,d}, d^{-1}$).

- ($Osat_{i,d}$ - $O_{i,d}$): The difference between the theoretical saturation concentration of oxygen ($Osat_{i,d}$) — the expected concentration if water and air were at equilibrium — and the actual concentration at time i on day d ($O_{i,d}$). This difference drives the exchange of oxygen with the atmosphere.

To estimate metabolism, I employed the **b_Kb_oipi_tr_plrckm.stan** variant within the StreamMetabolizer R package, adhering to the methodology and statistical procedures outlined by Appling et al. (2018a). The StreamMetabolizer package Appling et al. (2018a) provides comprehensive tools for analyzing stream metabolism. This variant's core equation models the change in oxygen concentration over time, incorporating daily parameters such as GPP, ER, and the gas exchange rate coefficient adjusted for the Schmidt number of 600 (K600). These parameters, alongside inputs like stream depth, photosynthetic photon flux density, and temperature-corrected gas exchange coefficients, facilitate a nuanced analysis of oxygen dynamics within aquatic environments.

This approach leverages a state space time series model to accommodate both observational and process errors, enhancing the accuracy of parameter estimation and reducing uncertainty. The adoption of the Bayesian Markov Chain Monte Carlo fitting procedure is essential for accurately determining the values of GPP, ER, and K600. This method allows me to finely tune the model to reflect observed oxygen concentrations and their variations with high precision, ensuring that my predictions remain closely aligned with actual biological processes and physical conditions in streams.

The days I continued to model were for Cornish Creek and Nancy Creek Johnson Ferry,

specifically between the years of 2017-2021, thus extending Appling et al. (2018b). Each site

had model parameters previously established by Appling. Both sites had 1000 burn-in steps to

get the model warmed up and an additional 500 runs saved. To further evaluate the model

results, the metric Rhat (Gelman-Rubin convergence statistic) was utilized. Appling et al.

(2018a) states that model performance significantly decreases when Rhat values exceed 1.20,

and modelers should aim to keep this value as close to 1.00 as possible. Cornish Creek and

Nancy Creek Johnson Ferry both had Rhat values between 1.00-1.03 for all model runs.

Furthermore, I employed partial pooling for K600 values across all days I modeled for each

site. Partial pooling of K600 is informed by a site-specific, piecewise linear relationship between

K600 and daily discharge, and addresses the complexity and variability inherent in stream

metabolism studies. This methodological choice, as Appling et al. (2018a) illustrates, mitigates

the risk of inaccurate parameter estimates, thereby improving overall model precision.

Additionally, further quality control checks removed all metabolism estimates that were

biologically impossible. This includes negative GPP or positive ER, or days where the 95% error

estimate of GPP or ER did not have the correct sign.

2.3   Depth and DO

Depth is one parameter in the Stream Metabolizer model, and was estimated from

discharge data from USGS National Water Information System (NWIS) and the "calc_depth"

StreamMetabolizer function. This function uses the equation $Z=cQ^f$, where Z is depth (m), c (m)

and f (unitless) are the regionalized hydraulic geometry coefficients, and Q is discharge (m^3 s^{-1})

Appling et al. (2018b). The "calc_depth" function fixes the coefficients in the above equation at

c=0.409 and f=0.294 which is based on a global regression Raymond et al. (2012). While long-

term discrete measurements of discharge and depth were accessible for all sites, offering an alternative approach for depth calculation, I opted for the Raymond et al. (2012) methodology to ensure uniformity across all sites and throughout the time series whenever regionalized hydraulic geometry coefficients were not present. The other key parameter for running StreamMetabolizer is the diel DO record, which was also retrieved at 15-minute intervals from the NWIS using the dataRetrieval package (DeCicco et al., 2024).

2.4 Characterizing and Grouping Watershed Land Cover

As an approximation for land use, I assumed land cover data would adequately represent the effects of anthropogenic influence via land use. To accomplish this, land cover for each watershed was characterized using the 2021 National Land Cover Database (Dewitz 2023). I used the open-source Geographic Information System (QGIS) software, alongside existing plugins such as the Watershed Stream Mapper tool. This tool generated a shapefile for each watershed at specified USGS stream gage locations. These watershed shapefiles were then overlaid onto the land cover data and clipped to match the boundaries of each watershed, creating specific land cover files.

I reclassified land cover into six categories: urbanization, agriculture, vegetation, water, wetlands, and other. This reclassification involved grouping land cover characteristics into three broad categories. Specifically, urbanization included 'Developed, High Intensity', 'Developed, Low Intensity', 'Developed, Medium Intensity', and 'Developed, Open Space'. Agriculture comprised 'Cultivated Crops' and 'Hay/Pasture', while vegetation included 'Deciduous Forest', 'Evergreen Forest', 'Mixed Forest', 'Shrub/Scrub', and 'Herbaceous'. Wetlands were categorized into 'Woody Wetlands' and 'Emergent Herbaceous Wetlands', and water was simply classified as 'Open Water'. Any land cover not fitting into these categories was classified as other. Using the

newly created land cover classifications, calculated as percentages, each watershed consisted of

at least 88% of either vegetation, urbanization, or agriculture (Table 2). This means that land

cover falling into the categories of water, wetlands, or other was largely excluded from further

consideration. Each site was then labeled as one of three categories: urbanization, even-mixed, or

vegetation. Sites characterized as urbanization had an urbanization percentage of at least 63%,

while those characterized as vegetation had a vegetation percentage of at least 50%. Sites

containing at least 25% of vegetation, urbanization, and agriculture were labeled as even-mixed.

Table 2: Site Watershed Characteristics
This table summarizes key watershed characteristics. It includes details on the state, RBI index, watershed area (in square miles), and land cover percentages (urban, vegetation, and agriculture) for each site.

Site	RBI	% Urban	% Vegetation	% Agriculture	Watershed area mi^2	Land Cover
Nancy Creek, GA	0.9602716	84.7	13.3	0.2	23.2	Urban
South River,GA	0.9307987	79.9	18.2	0.4	23.2	Urban
Intrenchment Creek, GA	0.8975408	83	13.6	2.3	10.9	Urban
Rocky R, NC	0.8659065	11.4	49.4	36	69.5	Vegetation
Proctor Creek	0.8356924	83.7	13.3	1.5	15.7	Urban
Nancy Creek RB, GA	0.7693709	84.4	13.8	0.2	28.1	Urban
Nancy Creek WW, GA	0.707486	79.1	19	0.5	37.5	Urban
NE Anacostia River, MD	0.6707848	63.3	24.1	6.9	75	Urban
Cornish Creek, GA	0.5391049	9.9	50.7	27.4	27.6	Vegetation
Enoree River, SC	0.3751936	26.4	52.2	15.6	445.1	Vegetation
Raritan River, NJ	0.3570739	26.4	39.6	24.9	491.8	Even Mixed
East Branch, PA	0.2852599	30.9	37.1	25.9	89.7	Even Mixed
Brandywine, PA	0.2736311	29.8	33.4	32.4	288.1	Even Mixed
West Branch, PA	0.2641431	28.3	33.3	34.1	55	Even Mixed

2.5   RBI Index

To better explain the relationship between watershed land cover and flow regimes I

calculated the Richards-Baker Flashiness Index (RBI). The Richards-Baker Flashiness Index

quantifies the variability or "flashiness" of discharge, indicating how rapidly a site responds to

rainfall events in terms of rising and falling water levels (Baker et al., 2004). The RBI is

calculated using daily streamflow data, the RBI then sums the absolute values of day-to-day

changes in streamflow and divides this by the total annual streamflow. A higher RBI suggests a

more flashy stream with rapid changes in streamflow, while a lower RBI indicates a more stable

stream with less variation. To provide a mechanistic link between land cover and stream

metabolism, sites were split into one of two groups based on their RBI value. If a site has an RBI

value above 0.60 it is considered flashy with sites having lower RBI values than 0.60, being

classified as non-flashy (Table 2).

Equation 2: Baker et al. (2004)

$$RBI = \frac{\sum |Q_i - Q_i - 1|}{\sum Q_i}$$

2.6   Selecting Hydrologic Flow Events

I wanted to identify storm events that were relatively isolated while also allowing for a

variety of storm events to occur. To achieve this, I calculated the percent change in the variation

of daily average discharge using the formula:

Equation 3: O'Donnell & Hotchkiss (2022)

$$(\frac{discharge_2 - discharge_1}{discharge_1}) \times 100$$

Where $discharge_1$ is the daily average discharge preceding $discharge_2$. For selection of a flow

event for further analysis, the criteria required that the percent change in daily variation of

average discharge remains below 40% for three consecutive days prior to the event, followed immediately by an event where the percent change exceeds 50%, which in turn is followed by another three consecutive days where the percent change once again falls below 40%. This threshold of up to 40% was chosen to better represent the hydrologic regimes across sites, particularly given the highly urbanized watersheds and the flashy flow regimes observed at some locations. This criterion also allowed the inclusion of a larger dataset of flow events for analysis. While the percent change in daily variation of average discharge can be used to isolate steady state conditions, I also calculated flow recurrence intervals to group the flow events. All events at a site that were isolated via the pre- and post- flow event criteria were ranked and put into quartile groups. This culminated in a total of 698 flow events, with each site having between 9-99 flow events (Table 1). This method was validated by visually inspecting the amount and type of storms at each site. Out of all the possible thresholds of change in average daily discharge for the pre – and post – event conditions, this method produced the widest variety of storm types and total storms across sites.

Out of the 14 sites, 12 have datasets of at least 10 years, with the other two sites having at least 7 years of data (Table 1). While it is possible that extreme flow events were not included in the flow recurrence intervals due to the flow duration curve being calculated during each site's data availability period, the length of the dataset mitigates this. However, it doesn't mitigate the possible impact of extreme changes in climate, which could influence the likelihood of a flow event occurring. This could result in wet periods or dry periods overlapping with the flow recurrence intervals, which would allow for events to shift up or down flow quartiles. Similarly, the distribution of flow events was an issue. I was able to record a multitude of flow events; however, the distribution of differing flow events across sites and seasons was not even. Some

sites had fewer events of varying storm sizes. However, this is largely mitigated by grouping

sites by their watershed land cover and avoiding site-to-site comparisons (Table 4). Additionally,

across all sites, there was no shortage of events in the uppermost quartile and lower third of

quartiles, allowing for the comparison of large events to smaller ones.

2.7   Calculating Resistance and Recovery

To calculate resistance, I utilized metrics previously developed by Reisinger et al. (2017)

and O'Donnell & Hotchkiss (2022). Considering the inherent day-to-day variability in GPP and

ER, I determined the mean antecedent metabolism using the average of estimates from the three

days prior to each flow event. To determine the stability of metabolism at baseflow and justify

the use of three-day averages, I calculated the coefficient of variation (CV) of daily metabolism

values during both baseflow and three-day periods of non-event conditions. The results showed

that while CVs were similar, the three-day metabolic averages had more occurrences with lower

CVs than baseflow periods, indicating greater stability (Appendix). This pattern was consistent

across all seasons and for both GPP and ER, suggesting that three-day averages provide a more

stable and representative measure of metabolism than seasonal baseflow means.

I assessed the metabolic responses to flow disturbances by comparing the pre-event

metabolic averages to the metabolic rates during and after the event. Resistance, specifically to

higher flow disturbances, was quantified by estimating the metabolic magnitude of departure (M)

for GPP and ER (Eq. 4) This was calculated for each flow event as the difference between the

event's GPP or ER (g O_2 m^{-2} d^{-1}) and the antecedent mean, designated as Xprior. To clearly

represent changes in stream productivity, I visualized increases in productivity as positive values,

and decreases as negative values, regardless of the directionality of the metric. Therefore, I

multiplied the resistance values for both ER and GPP by -1. This adjustment ensures that an

increase in ER, even though it results in more negative values, is visualized positively, aligning with increases in GPP. Similarly, decreases are visualized negatively, simplifying the interpretation of my results.

Equation 4: O'Donnell & Hotchkiss (2022)
$$M = 1 - X\_event/X\_prior$$

To evaluate the recovery of GPP and ER, I measured the recovery intervals (RIs), defined as the duration, in days, required for metabolic rates to revert to or surpass the average GPP or ER observed prior to the event, indicative of a re-establishment of the original environmental conditions. If metabolism data was missing for any days when calculating the recovery intervals, or if the metabolism never returned to pre-event conditions the flow event was excluded. This method for determining recovery follows the approach implemented by O'Donnell & Hotchkiss (2022). 15% of all events were removed due to their inability to return to pre-event conditions. This was largely due to the size of the dataset, which allowed for a multitude of scenarios where metabolism data was either unavailable or influenced by hydrologic conditions during recovery. Therefore, I opted to remove those days to avoid over-estimating the time of metabolic recovery.

2.8   Statistical Analyses

To answer the first portion of each of my hypotheses, assessing if there is a relationship between resistance and recovery to the size of storms, I compared the resistance and recovery values to the size of the flow events by using the four quartile groupings of storm event size. I used the Kruskal-Wallis test with a statistical threshold of $p = 0.05$ to test for differences in response (i.e., resistance and recovery) between storm event groups. This test determines if at least one group is significantly different than another, with groups being one of the flow quartiles in this example. This was performed for resistance and recovery of GPP and ER. If the Kruskal-Wallis test resulted in p-values less than 0.05, that indicates at least one group differs, and the

Wilcoxon two-sided rank sum test with the Bonferroni adjustment and a statistical threshold of p

= 0.05 was used to determine which flow quartiles were significantly different from each other.

To answer the second portion of my hypothesis, which is that land cover can influence how

resistant or resilient metabolism is to varying flow events, I tested the relationship between

resistance and recovery and the land cover categories as well as the RBI flashiness groupings

using the same statistical approach.

3   RESULTS

3.1   Overall Patterns

Across all sites I see that high metabolic productivity is related to high dissolved oxygen concentrations. Watersheds grouped by land cover had similar median dissolved oxygen and metabolism rates within each group (Table 3). Sites in the even-mixed watershed have some of the highest median DO levels and some of the highest median GPP. Urban sites typically have median DO and GPP values that fall between the even-mixed and vegetated watersheds (Fig. 3). The exception for median urban metabolism rates is ER, which has the highest median value out of the three watershed groupings. The vegetated watersheds all have very low rates of GPP and high rates of ER. These groupings by land cover become even more distinct when looking at net ecosystem production (NEP, Table 3). All sites are heterotrophic but to varying degrees. The even-mixed sites are the least heterotrophic and contain multiple sites that are almost autotrophic, the urban sites are more heterotrophic than the even-mixed sites, and the vegetated sites are strongly heterotrophic showing large rates of ecosystem respiration.

Table 3:A Comparative Analysis of Daily Dissolved Oxygen and Metabolism Metrics Across Sites and Grouped by Watershed Land Cover.
Median, range, and standard deviations for daily DO levels and metabolism rates (GPP, ER, NEP) are summarized for various sites under 'Even-mixed', 'Urban', and 'Vegetated' land cover categories. The table emphasizes the differences in stream metabolism associated with different

types of land cover, highlighting the ecological responses across a spectrum of environmental conditions.

| Land Cover	Site	Daily DO (mg/L)		Daily Metabolism (g O_2 m^{-2} d^{-1})		
		Median	range	GPP	ER	NEP
Even Mixed	East Branch	9.35 ± 1.55	$6.18 - 14.18$	3.76 ± 2.68	-5.09 ± 2.55	-0.94 ± 2.48
	Brandywine	9.31 ± 1.55	$6.62 - 14.55$	2.86 ± 1.91	-3.45 ± 1.80	-0.46 ± 1.95
	West Branch	9.46 ± 1.45	$6.81 - 15.07$	3.07 ± 2.70	-3.52 ± 1.69	-0.17 ± 2.32
	Raritan River	9.48 ± 1.98	$5.50 - 16.12$	3.70 ± 2.84	-3.93 ± 2.46	-0.06 ± 2.32
Urban	Nancy Creek	7.65 ± 1.37	$5.90 - 13.08$	0.59 ± 0.55	-1.52 ± 1.30	-0.75 ± 1.14
	Nancy Creek RB	8.15 ± 1.72	$3.77 - 13.62$	0.79 ± 0.75	-3.13 ± 2.29	-2.17 ± 1.99
	Proctor Creek	8.59 ± 1.66	$3.47 - 13.87$	1.46 ± 1.31	-2.73 ± 1.68	-1.02 ± 1.37
	Intrenchment Creek	7.31 ± 1.58	$3.44 - 13.21$	1.17 ± 1.19	-3.44 ± 2.87	-1.97 ± 2.61
	South river	7.29 ± 1.39	$4.53 - 12.07$	0.56 ± 0.37	-4.43 ± 2.40	-3.82 ± 2.33
	Nancy Creek WW	8.48 ± 1.62	$5.89 - 13.95$	0.82 ± 0.76	-3.01 ± 1.59	-1.94 ± 1.48
	NE Anacostia River	9.39 ± 1.89	$4.15 - 14.78$	2.71 ± 1.79	-3.70 ± 2.17	-0.85 ± 2.08
Vegetated	Enoree River	8.22 ± 1.47	$6.41 - 13.27$	0.71 ± 1.32	-5.70 ± 2.32	-4.51 ± 2.11
	Rocky R	6.72 ± 2.83	$1.10 - 13.08$	0.81 ± 0.75	-7.82 ± 4.41	-6.68 ± 4.32
	Cornish Creek	7.77 ± 1.52	$4.76 - 11.24$	0.24 ± 0.30	-2.14 ± 1.72	-1.89 ± 1.58
Values by land use	Even Mixed	9.39 ± 1.66	$5.50 - 16.12$	3.34 ± 2.60	-3.96 ± 2.30	-0.42 ± 2.33
	Urban	8.34 ± 1.79	$3.44 - 14.78$	1.03 ± 1.38	-3.08 ± 2.18	-1.60 ± 2.07
	Vegetated	7.68 ± 2.37	$1.10 - 13.27$	0.66 ± 0.99	-5.64 ± 3.99	-4.53 ± 3.7
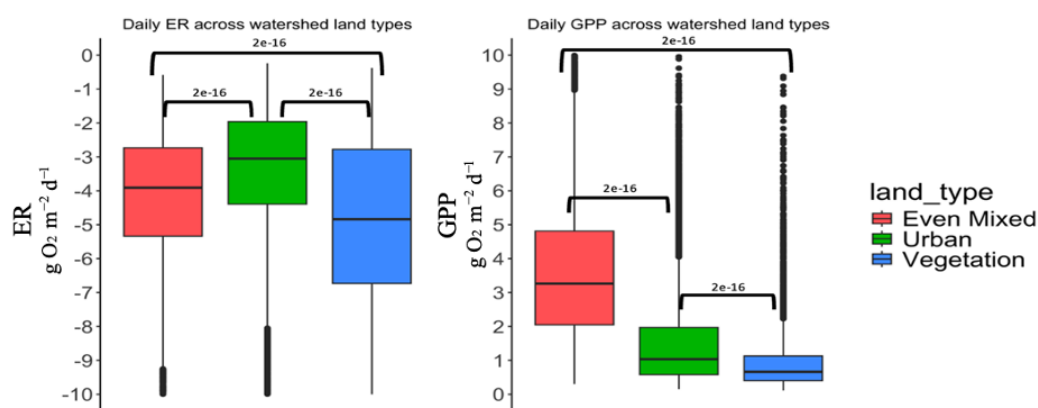
Figure 3:Daily Ecosystem Respiration and Gross Primary Production by Land Type
This figure illustrates the variation in daily ER and GPP across three land cover types: even-mixed, urban, and vegetation, using the entire dataset. The box plots display the median, interquartile range, and outliers. ER values are shown on the left, while GPP values are on the

right. Significant differences (p < 0.05, indicated by "bracketed values above the comparisons) between land types highlight the impact of land cover on ecosystem metabolism rates.

3.2   Resistance and Recovery across Flow

Median GPP resistance to storms ranged from -0.08 for small storms to -0.24 for large storms, while median ER resistance ranged from 0.12 for small storms to 0.03 for large storms (Table 4). Metabolic resistance across the four defined flow categories—below 25th percentile, 25th to 50th percentile, 50th to 75th percentile, and above the 75th percentile—varied for GPP but not ER (Table 4). GPP resistance exhibited statistically significant differences between the resistance to highest flows and each of the lower three quartiles (Fig. 4, p=0.00028, p=0.00035, and p=0.01529 when comparing above the 75th percentile to 50-75, 25-50, and below 25 respectively). GPP resistance to high flows was lower than the other flow categories. Conversely, I did not find statistically significant variations in ER resistance across these flow categories (Fig. 4).

Table 4:Median Resistance and Recovery of GPP and ER in Response to Storm and Flood Events Across Watershed Types and Watershed Flashiness.
This table presents the median resistance of GPP and ER to storms and the median recovery times (± standard deviation) to floods for each watershed type and flow event. It also includes flood stimulation data, which indicates the frequency with which flow events enhanced GPP or ER, shown as a count and percentage of the total floods analyzed per group. For flood stimulations, the larger number on the numerator above the percentage is the total amount of storms that occurred for each category.

	Resistance		Recovery(d)		Flood stimulation	
	GPP	ER	GPP	ER	GPP	ER
Even-mixed	-0.22	0.02	2 ± 4.44	0 ± 4.48	65/299 21%	157/299 52%
Urban	-0.11	0.10	0 ± 3.13	0 ± 2.22	117/302 38%	190/302 62%
Vegetated	-0.16	0.10	1 ± 2.27	0 ± 1.82	41/97 42%	51/97 52%
Flashy	-0.11	0.10	0 ± 3.10	0 ± 2.18	127/336 38%	201/336 62%
Non-Flashy	-0.22	0.02	2 ± 4.32	0 ± 4.34	170/362 47%	192/362 53%
Below 25th	-0.08	0.12	0 ± 4.29	0 ± 2.01	20/51 39%	32/51 62%
25th – 50th	-0.14	0.08	1 ± 3.58	0 ± 2.30	43/123 34%	76/123 61%
50th – 75th	-0.10	0.04	1 ± 4.79	0 ± 5.24	74/203 36%	120/203 59%
Above 75th	-0.24	0.03	1 ± 2.88	0 ± 2.32	86/321 26%	170/321 52%

To further explore the resistance differentiation in response to flow events, I consolidated the data into two groups: those below the 75th percentile and those above. After doing so the discrepancy in GPP Resistance was starkly evident, marked by strong significance ($p = 2.1e-07$), while the ER Resistance remained statistically insignificant ($p = 0.07$, Fig. 5). These results indicate that GPP is more strongly influenced by flow while ER seems to be controlled by other variables.

Median GPP recovery to storms ranged from 1 day for large storms to 0 days for small storms, while median ER recovery was 0 for all storm sizes (Table 4). Similarly, to resistance, metabolic recovery across the four defined flow categories—below 25th percentile, 25th to 50th percentile, 50th to 75th percentile, and above the 75th percentile—varied for GPP but not ER. Although GPP recovery was slightly different across flow quartiles it was not statistically significant (Fig. 6). Only after consolidating flow into either the uppermost or the lower three quartiles did I observe a statistically significant difference (Fig. 7, $p = 0.00924$ GPP recovery,

when comparing above the 75th quartile to the consolidation of lower quartiles). GPP recovery

from high flows was lower (slower) than the smaller flow group. Conversely, I did not find

statistically significant variations in ER recovery across these flow categories or after

consolidating flow into two groups (Fig. 7, p = 0.08751 ER recovery). To further assess how

recovery is related to anthropogenic influences I plotted median GPP and ER recovery values

against the four flow quartiles for each watershed land cover type (Fig. 8). Results reemphasize

the findings of the recovery box plots in (Fig. 6), which is that GPP and ER recovery are driven

by variables other than flow due to the wide variety of responses across watershed types and

flow quartiles.
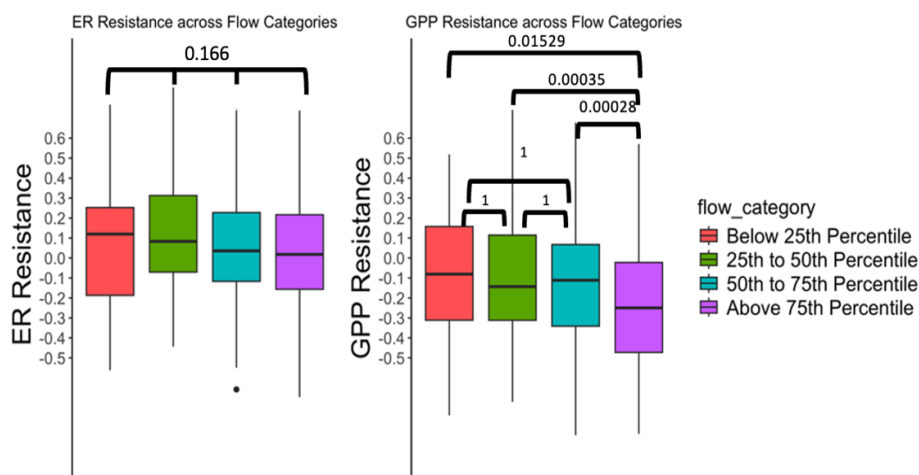
Figure 4:Resistance of ER and GPP Across Flow Categories.
Illustrates the resistance of ecosystem respiration (ER) and Gross Primary Production (GPP) to varying flow conditions, categorized by percentile ranges. The box plots compare the resistance metrics across four flow categories: below 25th percentile, 25th to 50th percentile, 50th to 75th percentile, and above 75th percentile. Resistance is expressed as medians, where values further from zero indicate a stronger metabolic shift due to flow events; positive values signify stimulation and negative values indicate suppression. Statistical significance between categories is marked for GPP, revealing differing impacts of flow intensity on production rates. Significant differences (p < 0.05, indicated by "bracketed values above the comparisons) between flow categories highlight the impact of flow on ecosystem metabolism rates.
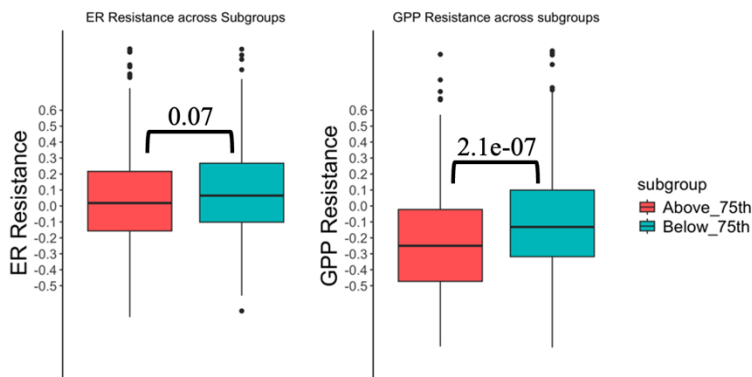
Figure 5:ER and GPP Resistance Across Subgroups Defined by Flow Intensity.
This figure depicts the resistance of ecosystem respiration (ER) and Gross Primary Production (GPP) to flow events, separated into subgroups above and below the 75th percentile of flow intensity. Resistance values closer to zero suggest minimal impact, whereas medians further from zero indicate a significant shift in metabolism due to flow events; positive resistance denotes stimulation and negative indicates suppression. The box plots show variability and outliers within each subgroup, and statistical significance is noted, with bracketed p-values indicating differences in GPP resistance between the subgroups.
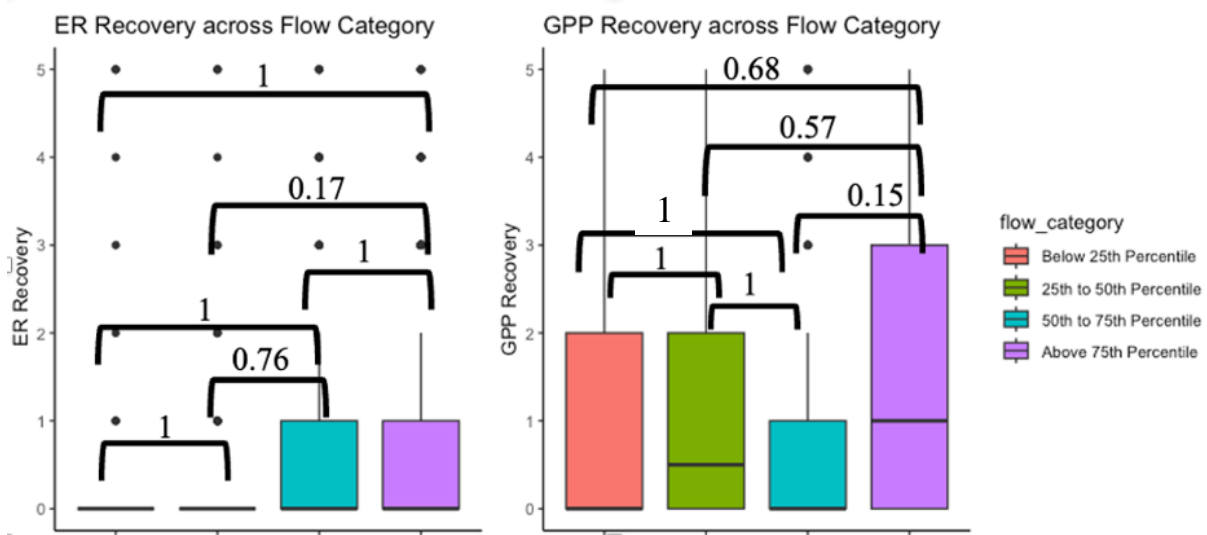

Figure 6:Recovery of ER and GPP across flow categories.
The recovery metrics of ecosystem respiration (ER) and Gross Primary Production (GPP) after flow events, categorized into four flow categories: below 25th percentile, 25th to 50th percentile, 50th to 75th percentile, and above 75th percentile. The recovery is measured by the time it takes for ER and GPP to return to baseline levels after a disturbance, with shorter recovery times indicating a more resilient ecosystem response. The box plots display variability within each subgroup, and significant differences in GPP recovery times are highlighted by the annotated bracketed p-values.
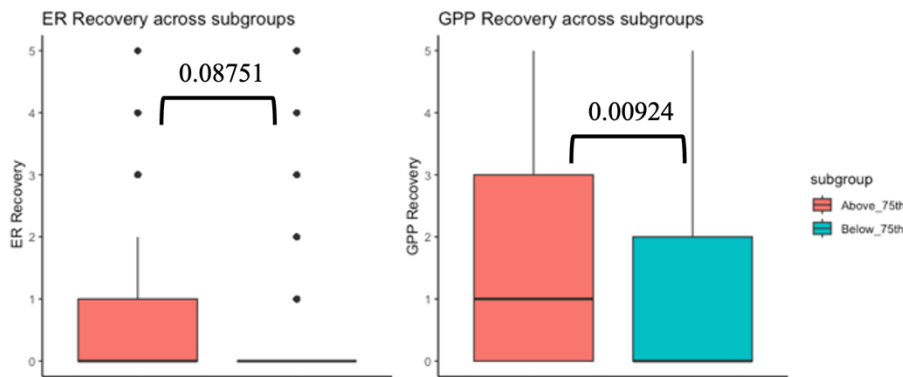
Figure 7:Recovery of ER and GPP in Subgroups Based on Flow Intensity.

The recovery metrics of ecosystem respiration (ER) and Gross Primary Production (GPP) after flow events, categorized into subgroups above and below the 75th percentile of flow intensity. The recovery is measured by the time it takes for ER and GPP to return to baseline levels after a disturbance, with shorter recovery times indicating a more resilient ecosystem response. The box plots display variability within each subgroup, and significant differences in GPP recovery times are highlighted by the annotated bracketed p-values.
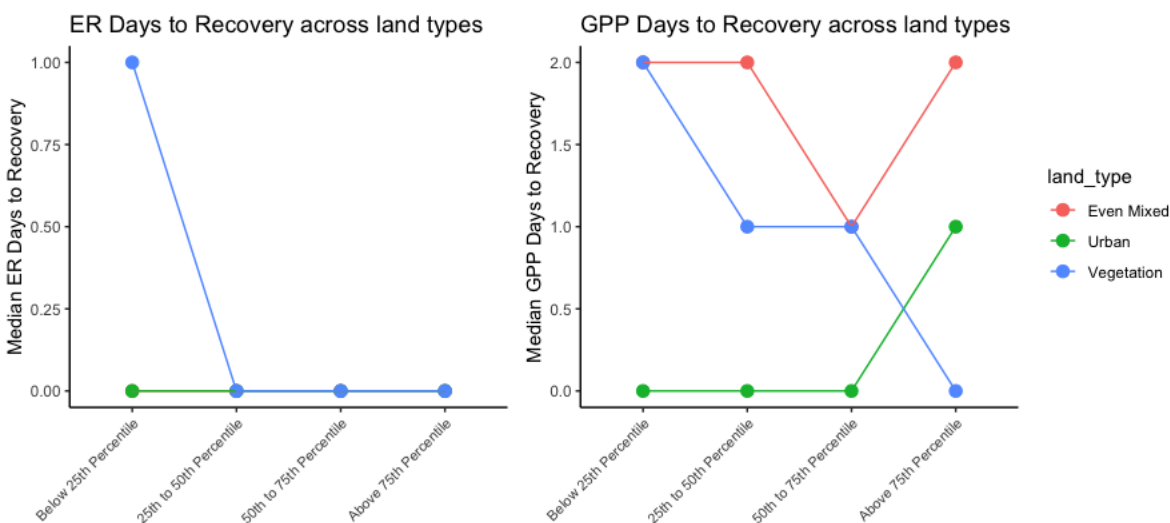
Figure 8:Median Recovery of ER and GPP Across Watershed Land Types and Flow Quartiles.

Median recovery times of ecosystem respiration (ER) and gross primary production (GPP) following environmental disturbances, across three watershed land types: even-mixed, Urban, and Vegetation. Recovery time is quantified by the duration needed for ER and GPP to return to pre-disturbance levels, with shorter times indicating a more resilient ecosystem. The scatter plots compare the median recovery times within each land type against the four flow quartiles.

3.3   Resistance and Recovery Across Land Cover

Median GPP resistance to storms ranged from -0.11 in urban watersheds to -0.16 in vegetated watersheds and -0.22 in even-mixed-use watersheds (Table 4). While median ER resistance ranged from 0.10 in vegetated watersheds, 0.10 in urban watersheds, and 0.02 in even-mixed-use watersheds. I found statistically significant differences for GPP and ER resistance between watersheds with mixed land cover and watersheds characterized by urbanization (p = 7e-06 for GPP resistance; p = 1e-05 for ER resistance, Fig. 9) with urban watersheds having higher resistance. However, I did not find any statistically significant differences between urban and vegetated watersheds, nor did I see any statistically significant differences between vegetated and even-mixed watersheds. Median GPP recovery was different for all watershed land cover types ranging from 0 days for urban watersheds, 1 day in vegetated watersheds, and 2 days for even-mixed watersheds (Table 4). Median ER recovery was 0 regardless of watershed land cover type. For metabolic recovery the only statistically significant differences were between the even-mixed watersheds in comparison to the urban watersheds (p = 2.1e-06 GPP recovery; p = 0.004 ER recovery, Fig. 10). I originally hypothesized (Fig. 1) that stream metabolism's resistance to disturbances decreases with increased anthropogenic land use and larger hydrologic disturbances. Plotting median resistance values against the four flow quartiles for each watershed land cover type indicates that GPP resistance does decreases in relation to flow disturbances across sites (Fig. 11). While GPP resistance does decrease, ER resistance is shown to increase often being stimulated by flow events regardless of flow event size or watershed land cover type (Fig. 11, Table. 4). Overall, I see that the even-mixed watersheds have the lowest resistance to flow events as well as take the longest to recover from flow events (Fig. 11, Fig. 10).
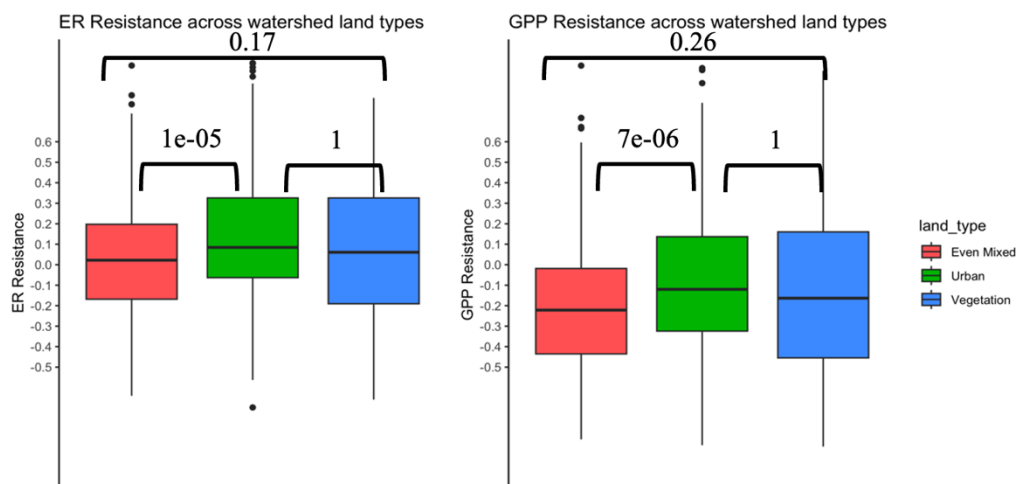
Figure 9:Resistance of ER and GPP Across Watershed Land Types.

Comparing the resistance of ecosystem respiration (ER) and gross primary production (GPP) across three watershed land types: even-mixed, urban, and vegetation. Resistance measures the deviation of ER and GPP from baseline conditions in response to environmental stressors, with positive values indicating stimulation and negative values indicating suppression. The box plots display the distribution of resistance values within each land type. Statistical annotations reveal significant differences in resistance patterns, particularly in GPP response between even-mixed and other land types. Significant differences ($p < 0.05$, indicated by the "bracketed values above the comparisons) between land types highlight the impact of land cover on ecosystem metabolism rates.
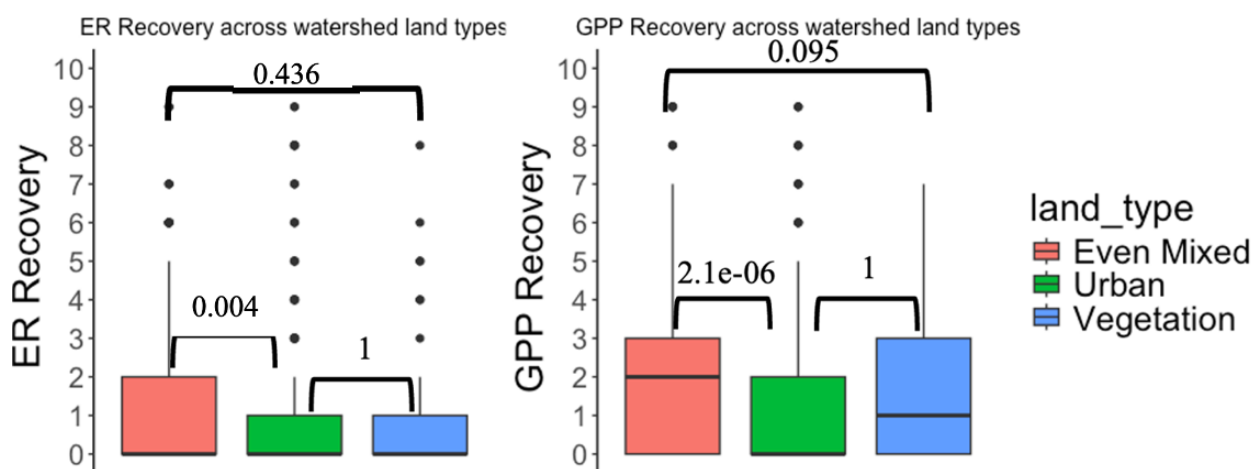
Figure 10:Recovery of ER and GPP Across Watershed Land Types.

The recovery times of ecosystem respiration (ER) and Gross Primary Production (GPP) following environmental disturbances, across three watershed land types: even-mixed, Urban, and Vegetation. Recovery time is quantified by the duration needed for ER and GPP to return to pre-disturbance levels, with shorter times indicating a more resilient ecosystem. The box plots reveal the range and distribution of recovery times within each land type. Statistically significant differences in recovery rates are highlighted, indicating varying resilience among land types.

Significant differences (p < 0.05, indicated by "bracketed values above the comparisons)
between land types highlight the impact of land cover on ecosystem metabolism rates.
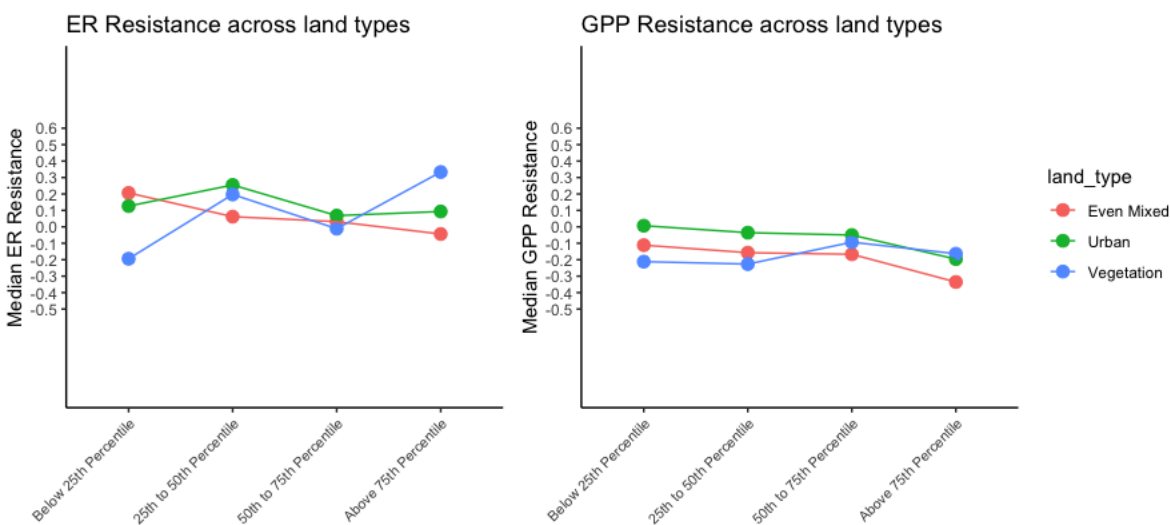
*Figure 11:Median Resistance values of ER and GPP Across Watershed Land Types and
Flow Quartiles.*
Comparisons of ecosystem respiration (ER) and gross primary production (GPP) resistance
across three watershed land types: even-mixed, urban, and vegetation. Resistance measures the
deviation of ER and GPP from baseline conditions in response to environmental stressors, with
positive values indicating stimulation and negative values indicating suppression. The scatter
plots show median resistance values for each site across each flow category.

3.4   Watershed Flashiness vs. Resistance and Recovery

The results of watershed flashiness in comparison to stream metabolism were very

similar to resistance and recovery across land cover. The median GPP and ER resistance for the

groups categorized as flashy was -0.11 and 0.10 with the non-flashy group having median GPP

and ER resistance values of -0.22 and 0.02 (Table 4). These resistance values are identical as the

watersheds characterized as urban and even mixed. This trend continues with recovery for GPP

and ER for between the flashy and non-flashy groups and the even-mixed and urban groups.

Further, the statistical significance between the flashy and non-flashy watershed groups and

resistance was strongly significant. (p = 9.1e-07 for GPP resistance; p = 1.1e-05 for ER

resistance, Fig. 12). Significant differences in watershed flashiness in comparison to GPP and ER

recovery were found as well (p = 6.4e-07 for GPP recovery; p = 0.0017 for ER recovery, Fig.

13). Ultimately, results show watersheds that are characterized as flashy are more resistant and

recover quicker to flow events than non-flashy watersheds.
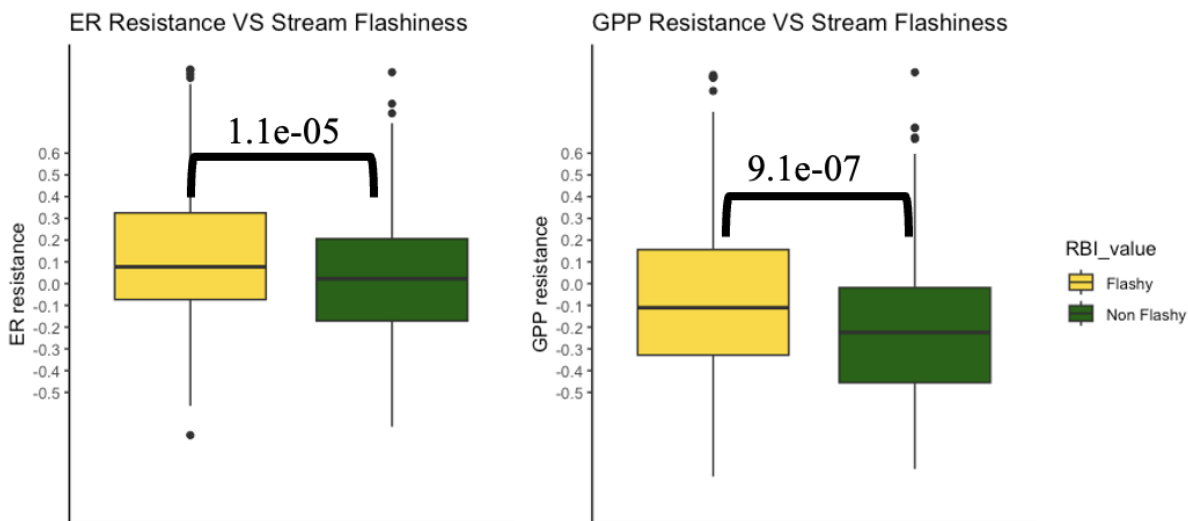
Figure 12:Resistance of ER and GPP against Watershed Flashiness
Compares the resistance of ecosystem respiration (ER) and gross primary production (GPP)
across watersheds deemed flashy or non-flashy. Resistance measures the deviation of ER and
GPP from baseline conditions in response to environmental stressors, with positive values
indicating stimulation and negative values indicating suppression. RBI measures how quickly a
watersheds hydrograph can change day to day. Watersheds that display volatile hydrographs
score higher on the RBI index and are considered flashy. The box plots display the distribution
of resistance values within each watershed type. Statistical annotations reveal significant
differences in resistance patterns in regard to sites classified as flashy. Significant differences (p
< 0.05, indicated by the "bracketed values above the comparisons) between land types highlight
the impact of land cover on ecosystem metabolism rates.
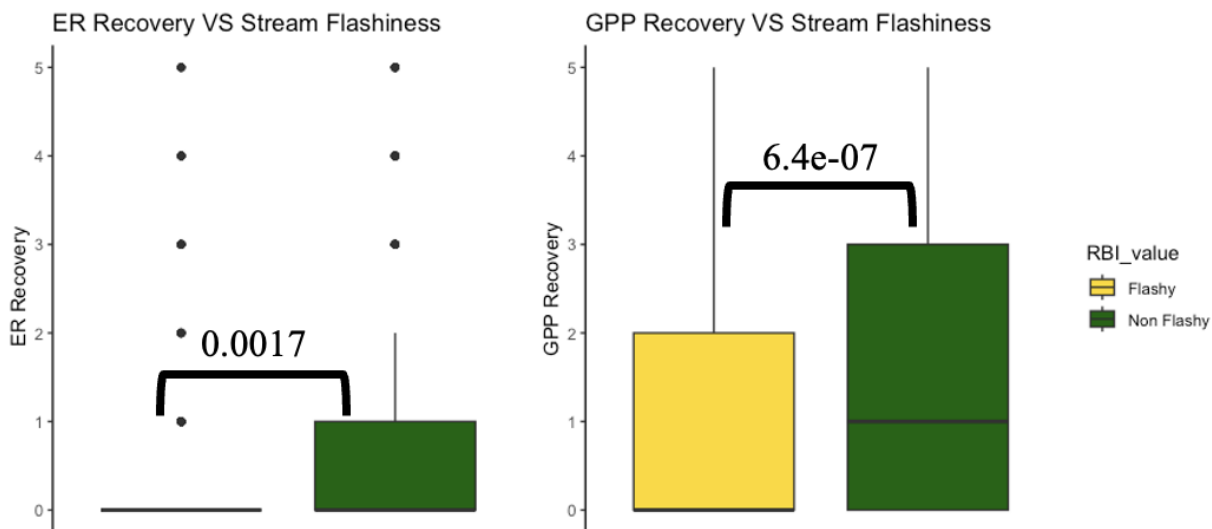
Figure 13:Recovery of ER and GPP against Watershed Flashiness.

Displays the recovery times of ecosystem respiration (ER) and Gross Primary Production (GPP) following environmental disturbances, across two watershed land types: Flashy or Non-Flashy. Recovery time is quantified by the duration needed for ER and GPP to return to pre-disturbance levels, with shorter times indicating a more resilient ecosystem. Flashiness is determined by the RBI index. Watersheds that scored high on the RBI were classified as flashy with others being non-flashy. The box plots reveal the range and distribution of recovery times within each watershed type. Statistically significant differences in recovery rates are highlighted, indicating varying resilience among land types. Significant differences ($p < 0.05$, indicated by "bracketed values above the comparisons) between watershed types highlight the impact of stream flashiness on ecosystem metabolism rates.

4   DISCUSSION

## 4.1   Variation in Metabolic Resistance with Flow Intensity

My hypothesis that there would be a negative correlation between resistance of stream

metabolism to disturbance events was partly correct. For GPP I found that flow events above the

75th percentile have lower resistance when compared to events of lesser magnitude (Fig. 5 and

Fig. 11). Specifically, flow events in the lower three quartiles have no significant statistical

differences to each other, but when comparing the lower three quartiles to the upper quartile,

significant differences appear (p = 2.1e-7 for GPP resistance; Fig. 5). Previous studies that

compared resistance to flow magnitude have had contrasting results. Both Qasem et al. (2019)

and Reisinger et al. (2017) found no relationship between flow event size and GPP or ER

resistance, while Griffiths et al. (2013) found a significant, negative relationship between GPP

resistance and the magnitude of change in discharge during flow events. Similarly to my

findings, Griffiths et al. (2013) found a relationship between resistance and flow only for GPP

and not ER. While ER resistance was not significant across flow quartiles, it did get closer to the

statistical threshold as flow event size increased (p = 0.07; Fig.5). This result is similar to

O'Donnell & Hotchkiss (2022) who observed that ER was more resistant than GPP across flow

events. The result of ER being more resistant than GPP indicates ER is likely responding

differently to storm events due to it being strongly influenced by organic material, and thus

might not be as immediately responsive to flow changes as GPP (Roberts et al., 2007, O'Donnell

& Hotchkiss 2022). Large flow events can easily disrupt the benthic layers where much of the

respiration activity occurs, but the overall impact may be buffered by the accumulation of new or

transported organic matter, which allows microbial consumption to continue even after

disturbance events. Furthermore, ER can be influenced by factors such as temperature and

dissolved oxygen levels, which may not vary directly with flow intensity in the short term (Bernot et al., 2010). This decoupling between ER and GPP during flow events suggests that ER's response mechanisms are more complex and perhaps moderated by longer-term ecological processes or legacies of previous disturbances.

4.2   Recovery Across Flow Categories

My analysis suggests that recovery in stream metabolism exhibits significant variations between flow extremes. Specifically, recovery metrics display marked differences when comparing the upper quartile of flow events with the lower third, with statistical significance observed in GPP responses (p = 0.0092) but not ER (p = 0.088). For both metrics larger storms result in lower recovery (longer recovery, Fig. 7). During high flow events, which are likely characterized by scouring processes, benthic materials are removed but may be offset by the influx of new organic materials. This dynamic could explain why even though GPP and ER show longer recovery times for larger storm events, ER's median recovery values are identical across the studied flow extremes (median RI = 0) which could also explain ER's statistical insignificance as well. Similarly, O'Donnell & Hotchkiss (2022) report multiple instances where ER recovery was 0 and their mean ER recovery was 1.1 days. Notably, the range of recovery times post-disturbance varies significantly between groups, with higher flows experiencing a quicker recovery range (0-24 days) compared to the lower flows (0-41 days). The quicker recovery times in the upper quartile may reflect the dual impact of physical disturbance—both clearing old benthic layers and introducing new organic substrates, which could facilitate faster metabolic recovery (Uehlinger 2006).

There is a possible bias in this data set due to the removal of events that did not return to pre-event conditions. The percentage of events that were removed were 15% of all events. To

address the issue of possible under estimation, the use of recovery rates regressed over time could remedy this issue. However, doing so comes with different limitations. Regressing recovery rates introduces situations where metabolism data may be decreasing after flow events, thus allowing for negative recovery times. Regressing recovery rates, also allows for events that never returned to pre-event conditions, which may have hit a new equilibrium to be interpreted as extremely long recovery times. Serious thought and consideration will be necessary to address the issue of possibly biased estimation of metabolism recovery times.

My findings extend the range of recovery times reported in previous studies, such as those by Reisinger et al. (2017) and Qasem et al. (2022), which documented recovery periods ranging from 4-18 days and 0.9-9.5 days. Reisinger et al. (2017) did not find a significant relationship between the size of the flow event and the time it takes to recover nor did Qasem et al. (2022). The broader range observed in this study underscores the influence of varying stream conditions and the scale of disturbance events. Overall, the recovery of stream metabolism to flow disturbances is influenced by both the intensity of the event and the pre-existing ecological conditions.

4.3   Land Cover Effects on Metabolic Responses

When accounting for land cover in my hypothesis, I observed that land cover is correlated to the metabolic responses of storm events for GPP resistance and recovery. Specifically, even-mixed watersheds exhibit distinctly different responses to storm events for resistance and recovery when compared to urban watersheds (Fig. 8, Fig.11, and Table 4). GPP in the even-mixed group has a lower resistance and recovery than the other watershed groups (even-mixed median GPP resistance = -0.22 and recovery = 2 days, Urban GPP median resistance = -0.11 and recovery = 0 days, Vegetated median resistance = -0.16 and recovery = 1

day; Table 4). When comparing GPP in the even-mixed watershed to another catchment with similar land cover characteristics, we do see some similarities; O'Donnell & Hotchkiss. (2022) observed a mean GPP resistance of -0.38 for large, isolated flow events in their mixed-use watershed. They also showed a similar average recovery interval with 2.5 days. However, if I compare an even-mixed catchment to a catchment that is dominated by agriculture, similarities decrease. Trentman et al. (2022) who focused on an agricultural dominated watershed, documented an average GPP resistance of -0.59 and a GPP recovery of 3.4 days. Although studies focusing on metabolism in agriculturally influenced or mixed-use watersheds are in short supply, I do see that GPP responds very differently depending on the amount of agriculture being practiced in a given catchment. These differences in agricultural land cover could explain the differing metabolic responses between Trentman et al. (2022)'s watershed which is 80% agriculture, and this studies agricultural watersheds which are less than 35% agricultural land cover.

Conversely to GPP, I see stronger similarities for ER resistance and recovery across land cover types (even-mixed median ER resistance = 0.02 and recovery = 0 days, Urban ER median resistance = 0.10 and recovery = 0 days, Vegetated ER median resistance = 0.10 and recovery = 0 days, Table 4). Often ER recovered quickly and was frequently stimulated across all land cover types, similar to that of Roley et al. (2014) and Qasem et al. (2022). When comparing ER resistance and recovery values across watersheds with significant agricultural influence, similarities are apparent. Notably, O'Donnell & Hotchkiss (2022) recorded an ER resistance of -0.09 and a recovery of 1.1 days, aligning closely with Trentman et al. (2022), who reported an ER resistance of -0.21 and a recovery of 2.7 days. Other studies in highly urban catchments also

found that ER is often more resistant and shows quicker recovery times in comparison to GPP as

well (Qasem et al., 2022, Reisinger et al., 2017).

      Surprisingly, the resistance for GPP and ER in urban watersheds were not statistically

different from those of vegetated watersheds (Fig. 9). This is surprising because other studies

focusing on urban sites show very different results from this study. Reisinger et al. (2017)

showed that urban streams in Baltimore Maryland have a very low resistance to flow events

(GPP resistance = -0.79 ER resistance = -0.72) and Qasem et al. (2022) showed metabolism in

urban streams in Chicago often increase after flow events (GPP resistance = 0.23 ER resistance =

0.80). Multiple factors could contribute to the lack of observed differences in GPP between

urban and vegetated watersheds, the first being baseline conditions. Analysis of baseline

metabolic activity by land cover shows that urban and vegetated watersheds have lower average

GPP compared to even-mixed sites (Fig. 3). Given that GPP is largely controlled by sunlight

exposure, this suggests that the urban and vegetated watersheds may share similar riparian

attributes. This is corroborated by the observation that both groups have low average GPP (Table

3), while the even-mixed group displays the highest average GPP. The lack of dissimilarities

between urban and vegetated watersheds could indicate that watershed-wide metrics of land

cover are not representative of canopy cover over streams (Bernot et al., 2010). My results show

that the group with the highest average GPP is the least likely to be stimulated by a storm event.

Taken together, this means baseline conditions are important and might strongly influence

metabolic resistance for GPP. This process is likely occurring due to the fact that sites with high

production have more producers to lose than they could gain during a given flow event.

However, it also suggests that the riparian vegetation, which would typically attenuate light, is

insufficient, thus not mitigating the impact of streambed scouring and habitat destruction.

It is also possible that a bias in watershed size is affecting the results. Six of the seven urban streams have a watershed area equal to or less than 37.2 mi^2 (Table 1). Watersheds larger than 37.2 mi^2 have different land cover classes and can be an order of magnitude larger. These differences in watershed size could be driving the results of his study and explain differences between land cover groups. Alternatively, if it is not the size of watersheds that is skewing land cover comparisons to metabolism, it could be watershed flashiness. While the majority of watersheds that are urban can be categorized as a small watershed, all urban watersheds in this study have RBI values above 0.60 (Table 2). The only site that is not urban with an RBI above 0.60 is the site Rocky R and is categorized as vegetated due to land cover percentages. This implies that stream flashiness and metabolism are influenced by land cover, but other factors are also at play. Studies show that variables contributing to stream flashiness include urbanization, road density, proximity to roads, and climate (Gannon et al., 2022). Although multiple studies have found inverse relationships between watershed size and flashiness at the regional scale (Baker et al., 2004, McPhillips et al., 2019), recent studies show that watershed size and flashiness are not correlated at the national scale (Gannon et al., 2022)

Interestingly, other studies of urban streams show no significant difference in metabolic recovery from my vegetated watersheds either. Reisinger et al. (2017) and O'Donnell & Hotchkiss (2022) have shown that urban streams often have high recovery or quick recovery times to storms, which is true for my study as well. However, my vegetated watersheds also show quick recovery times which is very different than Uehlinger (2006). Uehlinger (2006) reported GPP recovery values between 15-25 days for a vegetated headwater catchment. The lack of significant statistical differences between my vegetated and urban watersheds might be an indication that the scale at which I analyzed land cover (e.g., watershed-scale metrics) might

not represent the spatial scale that influences metabolism and storm response. This could be

remedied by incorporating a riparian metric or by assessing land cover at a more granular scale.

5   CONCLUSION

The goal of this study was to assess the recovery and resistance of GPP and ER to storms across watersheds in the Piedmont region. I hypothesized that there would be a negative relationship between resistance of stream metabolism to disturbance events and anthropogenic land cover. I observed that GPP exhibits significant resistance to high-flow events, particularly in even-mixed watersheds where such disturbances often lead to suppressed metabolic activity. Conversely, ER shows a varied response, indicating a recovery that is less influenced by flow events and more by the ecological characteristics and legacy effects within the watershed. This study underscores the complex dynamics between hydrologic events, land cover, and stream metabolism, offering novel insights into aquatic ecosystem dynamics.

My study bridges gaps in understanding the nuanced impacts of land cover on stream metabolism. The findings suggest that even-mixed watersheds, with their diverse land cover, often display the highest baseline metabolic rates, making them more responsive to storm events. I hypothesize the extent of riparian vegetation is possibly the strongest factor in mitigating the effects of hydrologic disturbances on metabolic processes. Notably, urban watersheds, while characterized by high recovery, did not exhibit significantly different recovery patterns from vegetated watersheds, hinting at the potential oversimplification of categorizing land cover types. These insights call for a more granular approach in future research, incorporating fine-scale land cover assessments and riparian metrics.

Ultimately, this research lays the groundwork for more refined management of aquatic environments. As long-term DO and discharge data become increasingly available, understanding the intricacies of stream metabolism across different watersheds will become easier. The knowledge gained from this study will inform future research and conservation

strategies aimed at quantifying the health of aquatic ecosystems. This will contribute to the shared goal of sustaining the integrity and functionality of stream ecosystems in the face of increasing disturbances.

REFERENCES

Alberts, J. M., Beaulieu, J. J., & Buffam, I. (2017). Watershed Land Use and Seasonal Variation

    Constrain the Influence of Riparian Canopy Cover on Stream Ecosystem Metabolism.

    Ecosystems, *20*(3), Article 3. https://doi.org/10.1007/s10021-016-0040-9

Andreadis, K. M., Brinkerhoff, C. B., & Gleason, C. J. (2020). Constraining the Assimilation of

    SWOT Observations With Hydraulic Geometry Relations. *Water Resources Research*,

    56(5), e2019WR026611. https://doi.org/10.1029/2019WR026611

Appling, A. P., Hall Jr., R. O., Yackulic, C. B., & Arroita, M. (2018a). Overcoming Equifinality:

    Leveraging Long Time Series for Stream Metabolism Estimation. *Journal of Geophysical*

    Research: Biogeosciences, *123*(2), Article 2. https://doi.org/10.1002/2017JG004140

Appling, A. P., Read, J. S., Winslow, L. A., Arroita, M., Bernhardt, E. S., Griffiths, N. A., Hall,

    R. O., Harvey, J. W., Heffernan, J. B., Stanley, E. H., Stets, E. G., & Yackulic, C. B.

    (2018b). The metabolic regimes of 356 rivers in the United States. *Scientific Data*, *5*(1),

    Article 1. https://doi.org/10.1038/sdata.2018.292

Atkinson, B. L., Grace, M. R., Hart, B. T., & Vanderkruk, K. E. N. (2008). Sediment instability

    affects the rate and location of primary production and respiration in a sand-bed stream.

    Journal of the North American Benthological Society, *27*(3), 581–592.

    https://doi.org/10.1899/07-143.1

Baker, D. B., Richards, R. P., Loftus, T. T., & Kramer, J. W. (2004). A NEW FLASHINESS

    INDEX: CHARACTERISTICS AND APPLICATIONS TO MIDWESTERN RIVERS

    AND STREAMS [1]. *JAWRA Journal of the American Water Resources Association*,

    40(2), 503–522. https://doi.org/10.1111/j.1752-1688.2004.tb01046.x

Bernhardt, E. S., Heffernan, J. B., Grimm, N. B., Stanley, E. H., Harvey, J. W., Arroita, M., Appling, A. P., Cohen, M. J., McDowell, W. H., Hall, R. O., Read, J. S., Roberts, B. J., Stets, E. G., & Yackulic, C. B. (2018). The metabolic regimes of flowing waters. *Limnology and Oceanography*, *63*(S1), Article S1. https://doi.org/10.1002/lno.10726

Bernhardt, E. S., Savoy, P., Vlah, M. J., Appling, A. P., Koenig, L. E., Hall, R. O., Arroita, M., Blaszczak, J. R., Carter, A. M., Cohen, M., Harvey, J. W., Heffernan, J. B., Helton, A. M., Hosen, J. D., Kirk, L., McDowell, W. H., Stanley, E. H., Yackulic, C. B., & Grimm, N. B. (2022). Light and flow regimes regulate the metabolism of rivers. *Proceedings of the National Academy of Sciences*, *119*(8), Article 8. https://doi.org/10.1073/pnas.2121976119

Bernot, M. J., Sobota, D. J., Hall Jr, R. O., Mulholland, P. J., Dodds, W. K., Webster, J. R., Tank, J. L., Ashkenas, L. R., Cooper, L. W., Dahm, C. N., Gregory, S. V., Grimm, N. B., Hamilton, S. K., Johnson, S. L., Mcdowell, W. H., Meyer, J. L., Peterson, B., Poole, G. C., Valett, H. M., … Wilson, K. (2010). Inter-regional comparison of land-use effects on stream metabolism. *Freshwater Biology*, *55*(9), 1874–1890. https://doi.org/10.1111/j.1365-2427.2010.02422.x

Bhaskar, A. S., Beesley, L., Burns, M. J., Fletcher, T. D., Hamel, P., Oldham, C. E., & Roy, A. H. (2016). Will it rise or will it fall? Managing the complex effects of urbanization on base flow. *Freshwater Science*, *35*(1), 293–310. https://doi.org/10.1086/685084

Blaszczak, J. R., Delesantro, J. M., Urban, D. L., Doyle, M. W., & Bernhardt, E. S. (2019). Scoured or suffocated: Urban stream ecosystems oscillate between hydrologic and dissolved oxygen extremes. *Limnology and Oceanography*, *64*(3), Article 3. https://doi.org/10.1002/lno.11081

Bott, T. L. (1983). Primary Productivity in Streams. In J. R. Barnes & G. W. Minshall (Eds.), *Stream Ecology* (pp. 29–53). Springer US. https://doi.org/10.1007/978-1-4613-3775-1_3

Clean Water Act of 1972, 33 U.S.C. §§ 1251-1387 (1972).

DeCicco, L., Hirsch, R., Lorenz, D., Watkins, D., & Johnson, M. (2024). dataRetrieval: R packages for discovering and retrieving water data available from U.S. federal hydrologic web services. https://doi.org/10.5066/P9X4L3GE

Dewitz, J., 2023, National Land Cover Database (NLCD) 2021 Products: U.S. Geological Survey data release, https://doi.org/10.5066/P9JZ7AO3.

Fellows, C. S., Clapcott, J. E., Udy, J. W., Bunn, S. E., Harch, B. D., Smith, M. J., & Davies, P. M. (2006). Benthic Metabolism as an Indicator of Stream Ecosystem Health. *Hydrobiologia*, *572*(1), 71–87. https://doi.org/10.1007/s10750-005-9001-6

Fuß, T., Behounek, B., Ulseth, A. J., & Singer, G. A. (2017). Land use controls stream ecosystem metabolism by shifting dissolved organic matter and nutrient regimes. *Freshwater Biology*, *62*(3), 582–599. https://doi.org/10.1111/fwb.12887

Gannon, J. P., Kelleher, C., & Zimmer, M. (2022). Controls on watershed flashiness across the continental US. *Journal of Hydrology*, *609*, 127713. https://doi.org/10.1016/j.jhydrol.2022.127713

Griffiths, N. A., Tank, J. L., Royer, T. V., Roley, S. S., Rosi-Marshall, E. J., Whiles, M. R., Beaulieu, J. J., & Johnson, L. T. (2013). Agricultural land use alters the seasonality and magnitude of stream metabolism. *Limnology and Oceanography*, *58*(4), 1513–1529. https://doi.org/10.4319/lo.2013.58.4.1513

Hill, W. R., Mulholland, P. J., & Marzolf, E. R. (2001). Stream Ecosystem Responses to Forest Leaf Emergence in Spring. *Ecology*, *82*(8), 2306–2319. https://doi.org/10.2307/2680233

Hoellein, T. J., Bruesewitz, D. A., & Richardson, D. C. (2013). Revisiting Odum (1956): A

synthesis of aquatic ecosystem metabolism. *Limnology and Oceanography*, *58*(6), Article

6. https://doi.org/10.4319/lo.2013.58.6.2089

Marzolf, Nicholas (2023). Estimates of ecosystem metabolism for 59 rivers in North America,
2008-2021 [Dataset]. Dryad. https://doi.org/10.5061/dryad.bcc2fqzj2

McPhillips, L. E., Earl, S. R., Hale, R. L., & Grimm, N. B. (2019). Urbanization in Arid Central

Arizona Watersheds Results in Decreased Stream Flashiness. *Water Resources Research*,

55(11), 9436–9453. https://doi.org/10.1029/2019WR025835

Mulholland, P. J., Fellows, C. S., Tank, J. L., Grimm, N. B., Webster, J. R., Hamilton, S. K.,

Martí, E., Ashkenas, L., Bowden, W. B., Dodds, W. K., Mcdowell, W. H., Paul, M. J., &

Peterson, B. J. (2001). Inter-biome comparison of factors controlling stream metabolism.

Freshwater Biology, *46*(11), 1503–1517. https://doi.org/10.1046/j.1365-

2427.2001.00773.x

O'Donnell, B., & Hotchkiss, E. R. (2022). Resistance and resilience of stream metabolism to

high flow disturbances. *Biogeosciences*, *19*(4), Article 4. https://doi.org/10.5194/bg-19-

1111-2022

Odum, H. T. (1956). Primary Production in Flowing Waters. *Limnology and Oceanography*,

1(2), Article 2.

O'Driscoll, M., Clinton, S., Jefferson, A., Manda, A., & McMillan, S. (2010). Urbanization

Effects on Watershed Hydrology and In-Stream Processes in the Southern United States.

Water, *2*(3), 605–648. https://doi.org/10.3390/w2030605

Qasem, K., Vitousek, S., O'Connor, B., & Hoellein, T. (2019). The effect of floods on ecosystem

metabolism in suburban streams. *Freshwater Science*, *38*(2), 412–424.

https://doi.org/10.1086/703459

Raymond, P. A., Zappa, C. J., Butman, D., Bott, T. L., Potter, J., Mulholland, P., Laursen, A. E., McDowell, W. H., & Newbold, D. (2012). Scaling the gas transfer velocity and hydraulic geometry in streams and small rivers. *Limnology and Oceanography: Fluids and Environments*, *2*(1), 41–53. https://doi.org/10.1215/21573689-1597669

Reisinger, A. J., Rosi, E. J., Bechtold, H. A., Doody, T. R., Kaushal, S. S., & Groffman, P. M. (2017). Recovery and resilience of urban stream metabolism following Superstorm Sandy and other floods. *Ecosphere*, *8*(4), Article 4. https://doi.org/10.1002/ecs2.1776

Roberts, B. J., Mulholland, P. J., & Hill, W. R. (2007). Multiple Scales of Temporal Variability in Ecosystem Metabolism Rates: Results from 2 Years of Continuous Monitoring in a Forested Headwater Stream. *Ecosystems*, *10*(4), 588–606. https://doi.org/10.1007/s10021-007-9059-2

Roley, S. S., Tank, J. L., Griffiths, N. A., Hall, R. O., & Davis, R. T. (2014). The influence of floodplain restoration on whole-stream metabolism in an agricultural stream: Insights from a 5-year continuous data set. *Freshwater Science*, *33*(4), 1043–1059. https://doi.org/10.1086/677767

Trentman, M. T., Tank, J. L., Davis, R. T., Hanrahan, B. R., Mahl, U. H., & Roley, S. S. (2022). Watershed-scale Land Use Change Increases Ecosystem Metabolism in an Agricultural Stream. *Ecosystems*, *25*(2), 441–456. https://doi.org/10.1007/s10021-021-00664-2

Uehlinger, U. (2000). Resistance and resilience of ecosystem metabolism in a flood-prone river system: Resistance and resilience of ecosystem metabolism. *Freshwater Biology*, *45*(3), Article 3. https://doi.org/10.1111/j.1365-2427.2000.00620.x

Uehlinger, U. (2006). Annual cycle and inter-annual variability of gross primary production and

    ecosystem respiration in a floodprone river during a 15-year period. *Freshwater Biology*,

    51(5), 938–950. https://doi.org/10.1111/j.1365-2427.2006.01551.x

Walsh, C. J., Roy, A. H., Feminella, J. W., Cottingham, P. D., Groffman, P. M., & Morgan, R. P.

    (2005). The urban stream syndrome: Current knowledge and the search for a cure.

    Journal of the North American Benthological Society, *24*(3), 706–723.

    https://doi.org/10.1899/04-028.1

Young, R. G., & Huryn, A. D. (1996). *Interannual variation in discharge controls ecosystem*

    metabolism along a grassland river continuum. *53*(10), 2199–2211.

    https://doi.org/10.1139/f96-186

Young, R. G., & Huryn, A. D. (1999). EFFECTS OF LAND USE ON STREAM

    METABOLISM AND ORGANIC MATTER TURNOVER. *Ecological Applications*,

    9(4), 1359–1376. https://doi.org/10.1890/1051-0761(1999)009[1359:EOLUOS]2.0.CO;2

Young, R. G., Matthaei, C. D., & Townsend, C. R. (2008). Organic matter breakdown and

    ecosystem metabolism: Functional indicators for assessing river ecosystem health.

    Journal of the North American Benthological Society, *27*(3), 605–625.

    https://doi.org/10.1899/07-121.1

APPENDICES

Appendix

Table 5: CV Results Quantifying Non-Event Flow Daily Metabolism Stability Across Seasons.
Displayed is the average coefficient of variation (CV) calculated for each site during each season for GPP and ER. CVs for daily metabolism were calculated at baseflow and during periods that qualified as pre-event conditions (Xprior). Out of the 56 entries in this table, GPP during Xprior had a lower CV than baseflow 35 times, while ER Xprior had a lower CV than baseflow 31 times indicating the methodology employed to capture pre-event metabolism is sufficient.

Site	Site land cover type	Season	Average CV for ER at baseflow	Average CV for GPP at baseflow	Average CV for ER at Xprior	Average CV for GPP at Xprior
East_Branch_Brandywine_Creek	Even Mixed	Fall	-51.42204	42.13289	-49.16284	42.65415
East_Branch_Brandywine_Creek	Even Mixed	Spring	-45.66797	56.44372	-45.11262	58.12181
East_Branch_Brandywine_Creek	Even Mixed	Summer	-34.71178	33.5061	-33.33345	36.30917
East_Branch_Brandywine_Creek	Even Mixed	Winter	-34.82929	67.23949	-28.31279	67.19643
Brandywine_Creek	Even Mixed	Fall	-45.29313	55.18518	-41.80036	55.17319
Brandywine_Creek	Even Mixed	Spring	-51.21358	48.73222	-48.67519	50.0722
Brandywine_Creek	Even Mixed	Summer	-33.43037	40.04716	-33.02471	43.56602
Brandywine_Creek	Even Mixed	Winter	-43.58069	92.64943	-48.57243	64.70162
West_Branch_Brandywine_Creek	Even Mixed	Fall	-38.34313	41.3622	-38.67447	39.96397
West_Branch_Brandywine_Creek	Even Mixed	Spring	-42.87538	50.87099	-46.1725	53.82874
West_Branch_Brandywine_Creek	Even Mixed	Summer	-29.05364	37.09874	-30.68323	36.50545
West_Branch_Brandywine_Creek	Even Mixed	Winter	-70.80162	56.94623	-46.44743	56.35096
Raritan_River	Even Mixed	Fall	-60.80517	62.16137	-53.61339	62.4448
Raritan_River	Even Mixed	Spring	-47.98133	52.12812	-41.83768	51.63394
Raritan_River	Even Mixed	Summer	-35.32694	44.99151	-36.15131	48.40525
Raritan_River	Even Mixed	Winter	-37.5233	74.63746	-45.48426	65.68572
Nancy_Creek	Urban	Fall	-46.60861	69.92499	-51.3163	71.27258
Nancy_Creek	Urban	Spring	-64.03223	55.46547	-69.78998	54.2435
Nancy_Creek	Urban	Summer	-61.89703	56.31151	-67.76552	58.81889
Nancy_Creek	Urban	Winter	-41.0645	49.45889	-57.13953	40.31682
Nancy_Creek_Rickenbacker	Urban	Fall	-61.11227	57.46252	-54.70003	53.64865
Nancy_Creek_Rickenbacker	Urban	Spring	-65.94086	60.84775	-57.77609	64.31642
Nancy_Creek_Rickenbacker	Urban	Summer	-51.32326	50.83772	-47.26507	47.38772
Nancy_Creek_Rickenbacker	Urban	Winter	-56.20656	59.26798	-47.54972	56.16257
Proctor_Creek	Urban	Fall	-58.61171	66.43694	-54.05496	63.21387
Proctor_Creek	Urban	Spring	-42.75204	44.91791	-35.96049	49.62465
Proctor_Creek	Urban	Summer	-51.1684	46.66929	-44.69594	47.11722
Proctor_Creek	Urban	Winter	-46.28729	66.30122	-39.96369	60.75595
Intrenchment_Cr	Urban	Fall	-49.06372	69.7395	-56.44273	64.71932
Intrenchment_Cr	Urban	Spring	-54.03995	73.73022	-48.61504	66.97763
Intrenchment_Cr	Urban	Summer	-67.64692	56.78869	-58.91958	55.12193
Intrenchment_Cr	Urban	Winter	-48.45714	67.46547	-48.84617	69.95061
South_River	Urban	Fall	-39.25034	48.26888	-38.64254	45.82816
South_River	Urban	Spring	-39.77829	51.60181	-40.20628	46.25326
South_River	Urban	Summer	-40.06532	44.3194	-43.12308	38.4298
South_River	Urban	Winter	-37.84264	56.10941	-38.55343	52.67049
Nancy_Creek_West_Wesley	Urban	Fall	-52.44139	55.88603	-46.07338	48.98666
Nancy_Creek_West_Wesley	Urban	Spring	-40.67433	57.59982	-35.35052	58.40039
Nancy_Creek_West_Wesley	Urban	Summer	-40.67465	46.38797	-35.48895	43.20657
Nancy_Creek_West_Wesley	Urban	Winter	-51.82046	68.02651	-45.4945	67.05817
Northeast_Branch_Anacostia_River	Urban	Fall	-42.13276	52.4224	-40.00381	52.86448
Northeast_Branch_Anacostia_River	Urban	Spring	-45.9299	38.73558	-48.92975	42.91238
Northeast_Branch_Anacostia_River	Urban	Summer	-31.04269	33.87274	-29.40411	36.44692
Northeast_Branch_Anacostia_River	Urban	Winter	-36.60916	49.42585	-38.59883	48.79724
Enoree_River	Vegetation	Fall	-31.21278	107.72929	-30.47364	100.27614
Enoree_River	Vegetation	Spring	-30.30703	54.39505	-31.09501	45.94866
Enoree_River	Vegetation	Summer	-23.33374	112.2763	-25.57888	104.04949
Enoree_River	Vegetation	Winter	-38.84986	64.22481	-50.61077	77.61956
Rocky_R	Vegetation	Fall	-39.85388	44.30032	-39.95799	41.8379
Rocky_R	Vegetation	Spring	-51.43775	73.53426	-50.92278	66.68777
Rocky_R	Vegetation	Summer	-36.8079	48.54127	-38.81555	43.3177
Rocky_R	Vegetation	Winter	-52.02544	88.24821	-47.85018	78.17805
Cornish_Creek	Vegetation	Fall	-27.78181	33.7485	-34.49427	37.48408
Cornish_Creek	Vegetation	Spring	-64.58055	81.00478	-65.88659	74.63569
Cornish_Creek	Vegetation	Summer	-34.7751	35.89553	-30.04431	22.44884
Cornish_Creek	Vegetation	Winter	-38.30115	59.94194	-79.76204	84.08503